Journal of Chromatography A, 1236 (2012) 51–62

Contents lists available at SciVerse ScienceDirect

Journal of Chromatography A

journal homepage: www.elsevier.com/locate/chroma

Multiple, simultaneous, independent gradients for versatile multidimensional liquid chromatography. Part I: Theory

Allen G. Hirsh*, Latchezar I. Tsonev

CryoBioPhysica, Inc., 8909 Ellsworth Ct., Silver Spring, MD 20910, USA

ARTICLE INFO

Article history:
Received 4 July 2011
Received in revised form 21 February 2012
Accepted 26 February 2012
Available online 6 March 2012

Keywords:
pISep
pH gradient ion exchange chromatography
Electrostatic interaction theory
pH gradient chromatography
multidimensional liquid chromatography
Proteomics
Protein purification

ABSTRACT

The general method for constructing coupled dual gradients in liquid chromatography (LC) is to begin by filling a reservoir A with a solution of one mobile phase (MP) component at concentration [c_1(A)] and a second MP component at concentration [c_2(A)], followed by filling a reservoir B with a solution containing MP component one at concentration [c_1(B)] and the second MP component at concentration [c_2(B)]. In another scenario the reservoirs A and B are filled with solutions of only one MP component at different concentrations [c_1(A)] and [c_1(B)] and the two solutions are titrated to a different pH value: pH (A) for the reservoir A and pH (B) for the reservoir B respectively. In either case, mixing of flows from the two reservoirs varies the concentrations of the two MP components (MP solutes) or the concentration of one MP component and pH along a particular compositional curve producing an eluent with two compositionally coupled gradients. This is a kind of a two dimensional LC utilizing dual simultaneous dependent gradients (DSDGs) wherein two parameters affecting the binding free energy of an analyte to a stationary phase (SP) are being altered simultaneously. Such a DSDG suffers from a significant limitation in that the gradient concentration of the two solutes or the concentration of one MP component and the pH cannot be varied independently. The only way to attain an optimal multigradient LC system, that promises a remarkable increase in chromatographic resolution of complex analyte mixtures, is to uncouple the multiple (dual) gradients, making each independent of the other(s). In this paper the theory of uncoupling of n such gradients, $n \geq 2$ is developed. It is shown that for n solutes 2^n reservoirs are required in concert with an LC eluent delivery system capable of freely apportioning the flows among the reservoirs according to equations we develop here. We go on to predict a substantial increase in chromatographic resolution when applying dual simultaneous independent gradients (DSIGs) of salt and pH to fractionate difficult to separate proteins. This prediction is naturally explained by the electrostatic interaction theory of protein binding to an ion exchanger. In subsequent experimental papers it will be shown that the algorithms presented here properly instruct a quad pump HPLC system to produce well controlled independent simultaneous gradients of pH and non-buffering solutes with attendant significant gain in chromatographic resolution of complex mixtures of protein isoforms.

1. Introduction

1.1. Background

Gradient chromatography greatly expands the resolution of LC as a separation technique by taking advantage of the fact that the partitioning of an analyte between a stationary phase and a mobile phase is quantified by the retention factor, k, which is exponentially dependent on the free energy of binding of the analyte to the stationary phase. Thus, modest changes in the chemistry of the mobile phase are capable of producing large changes in k. In gradient LC this is easily exploited to provide differences in the time integrated movement on a stationary phase of two chemically very similar analytes, whereas their movement on the same stationary phase would be nearly identical under isocratic conditions. Most often the gradient is a time dependent change in the concentration of one component of a MP that is effective in altering analytes' binding to a stationary phase, e.g. NaCl in ion exchange (IEX) or acetonitrile in reversed phase (RP) LC. Additionally, in ion exchange chromatography it is generally understood that a properly controlled pH gradient should provide significantly better resolution of charged macromolecules than a gradient of increasing ionic strength at isocratic pH, and this was the basis for Sluyterman's development of chromatofocusing [1–5]. Since then there have been numerous attempts to provide a reliable, more flexible method of generating well controlled wide ranging pH gradients on

* Corresponding author. Tel.: +1 301 908 0288; fax: +1 240 399 0518.
E-mail address: agh@cryobiophysica.com (A.G. Hirsh).

0021-9673/$ – see front matter © 2012 Elsevier B.V. All rights reserved.
doi:10.1016/j.chroma.2012.02.072

both cationic and anionic stationary phases [6–17], but only with the advent of the pISep system has the problem been essentially solved [18,19]. In pISep chromatography mixing of two buffers, water solutions of 4 mM piperazine, 4 mM N-methylpiperazine, 4 mM triethanolamine, 4 mM bis–tris propane and 2 mM formic acid, one titrated to a highly alkaline pH and the other to a very acidic pH has been shown to allow formation of highly controllable and reproducible pH gradients on cationic, anionic, mixed mode and mixed bed SPs over up to a 10 pH unit range.

Nevertheless, it is usually more efficient to change two MP chemistries simultaneously because that increases the probability of differences in the k values of chemically similar analytes throughout the evolution of the gradient. As presently constituted, a typical coupled (dependent) dual salt and pH gradient might, e.g., go from 0 to 200 mM salt while simultaneously going from pH 6.87 to pH 6.57 using 10 mM bis–tris buffer [20]. In this example if two proteins, hemoglobin isoforms, have virtually the same binding free energy to an ion exchanger at pH 6.87, separation by a salt gradient at isocratic pH 6.87 will cause them to co-elute at the same salt concentration. In contrast, differences in the titration curves of the two hemoglobin isoforms will cause their k values to diverge as a consequence of a pH change during a coupled dual pH-salt gradient separation on the same ion exchanger and as a result they can often be resolved from each other. These DSDGs are generally formed in a straightforward way using mobile phases with water as a solvent. A first reservoir, call it A, is filled with a buffer solution at a desired pH without or with a minimum salt concentration. A second reservoir, call it B, is filled with the buffer solution at a different pH containing the maximum salt concentration. The two dependent salt and pH gradients are then formed by proportional mixing of the solutions from the two reservoirs over time using a binary LC gradient system. By utilizing aqueous buffer solutions containing salt over short pH ranges wherein a given buffering compound is near its pK_a throughout the pH range of the dual coupled gradient, one can expect that the pH will change along a gradient curve shaped roughly like that of the salt gradient curve (usually linear) as programmed by the chromatographer. The same kind of DSDG can be generated in RP LC by utilizing solutions of water and miscible organic solvents at differing pH values and this has been studied in some detail [21–24]. Thus, as presently used in both binary and quaternary gradient pump chromatography dual gradient LC is an example of a limited, coupled kind of dual gradient technology because two parameters, each of which contributes independently to the strength of binding of an analyte to a stationary phase, are being varied simultaneously but not independently of each other. Dual gradient LC techniques, when achievable, are to be preferred. The analysis below makes this clear. In the case where the local interactions of the analytes to be separated with the stationary phase include a significant hydrophobic (Van der Waals) component in concert with strong electrostatic interactions, i.e. mixed mode interactions, the free energy differences determining k are additive as exponents. This can be stated formally by explicitly comparing the free energy of binding of two analytes separated in tandem by, e.g. IEX followed by RP to the same two analytes separated by a chromatographic system utilizing the same two methods simultaneously:

$\left(\frac{k_{1,IEX}}{k_{2,IEX}}\right) = \Phi_{IEX}\, e^{\frac{\Delta G_{2,IEX}-\Delta G_{1,IEX}}{RT}}$ first dimension of a standard sequential separation where $\Delta G_{1,IEX}$, $\Delta G_{2,IEX}$ = electrostatic binding free energy of analytes 1 and 2 respectively, and

$\left(\frac{k_{1,RP}}{k_{2,RP}}\right) = \Phi_{RP}\, e^{\frac{\Delta G_{2,RP}-\Delta G_{1,RP}}{RT}}$ second dimension of the sequential separation where $\Delta G_{1,RP}$, $\Delta G_{2,RP}$ = Van der Waals binding free energy of analytes 1 and 2, respectively

In the case of a dual gradient separation the expression would be:

$$\left(\frac{k_{1,RP+IEX}}{k_{2,RP+IEX}}\right) = \Phi_{RP+IEX}\, e^{\frac{([\Delta G_{2,IEX}+\Delta G_{2,RP}+\Delta G_{2,RP+IEX}]-[\Delta G_{1,IEX}+\Delta G_{1,RP}+\Delta G_{1,RP+IEX}])}{RT}}$$

Thus, it is much more likely for the mobile phase to invoke a significant difference between the retention factors of the two analytes at any given point in the gradient when two free energies of interaction of the analytes with the stationary phase, the hydrophobic and the electrostatic, are altered simultaneously as in this example.

As useful as such DSDG LC techniques are, one can envision much more versatile and powerful dual gradient systems in which the gradients of two MP components or one MP component and pH are uncoupled and therefore independent of each other [2]. We call this class of LC gradients dual simultaneous independent gradients (DSIGs) illustrated and compared to DSDGs in Fig. 1. In the right-hand column of panels (E–H), the x axis represents the concentration of one MP component, the y axis pH or the concentration of a second MP component. As illustrated in these panels, in the DSDGs the composition profile of the mobile phase always changes along a particular compositional curve in the x–y plane as the proportions of solutions pumped from reservoir 1 and reservoir 2 are varied. For linear proportioning and mixing of two component solutions it is always a straight line, but for one non-buffering MP component and pH it usually has at least some curvature. In contrast, in DSIGs LC the entire x–y compositional plane is accessible for formation of gradient elution profiles composed of two compositionally independent gradients. In a mathematical sense this means that the compositional profile of the mobile phase in time could, in theory, follow any continuous compositional curve in the x–y plane bounded by the compositional limits of the fluids in the reservoirs, and subject to the volume delivery limits of the quad LC pumping system.

Ipso facto, that represents a very large increase in the simultaneous, selective control of the various forces causing the binding of analyte molecules to stationary phases, and thus chromatographic selectivity and resolution.

1.2. Goals

In this paper we have four theoretical goals: (1) to define the mathematics for creating DSIGs of two MP components, i.e. independent (decoupled) gradients in the composition of each of the compounds in the mobile phase; (2) to define the mathematics for a special class of DSIGs in which one of the independent gradients is in the composition of a non-buffering MP compound and the other is in pH over a wide pH range, utilizing the pISep computer controlled pH gradient formation system [6], with the acronym DSIGspH; (3) to define algorithms that generalize the DSIGs system to n compounds, multiple simultaneous independent gradients MSIGs) or the DSIGspH system to $n-1$ compounds and pH (MSIGspH); and (4) to demonstrate some of the advantages of DSIGspH over both salt gradients at isocratic pH and DSDGs by numerical integration of the binding equations of the modern electrostatic interaction theory (EI) of IEX LC [3–6].

In subsequent experimental papers we will show that the DSIGspH equations developed here (see below) are applicable in practice and successfully calculate LC protocols for generating dual independent gradients of non-buffering MP additives (MP solutes) and pH (e.g. NaCl and pH, urea and pH or acetonitrile and pH) by a quaternary pump HPLC system. We will demonstrate that the composition of each of the two uncoupled gradients can be accurately, simultaneously and independently varied and controlled

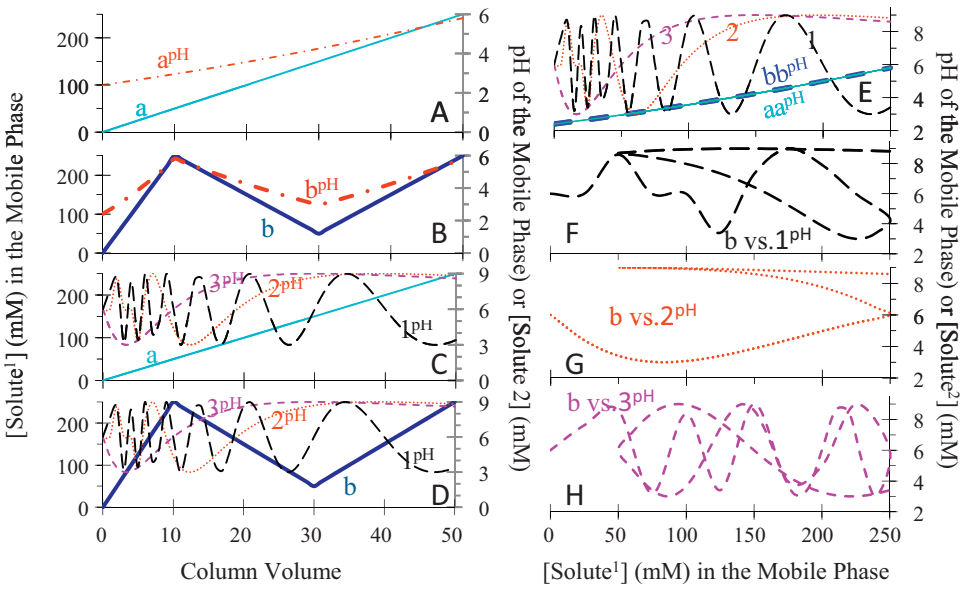

Fig. 1. Gradient profiles (panels A–D) and compositional profiles (panels E–H) of LC DSDGs and DSIGs. Solute refers to non-buffering mobile phase component, not analyte. (A) Cyan line a – one step linear DSDG of solute[1] and its dependent pH gradient – red dash dotted line a^{pH}. (B) Solid dark blue solid curve b – linear three step DSDGs of solute[1] and its dependent pH gradient–dash dotted dark red curve b^{pH}. (C) Three DSIGs consisting of the same one step linear salt gradient (cyan curve a, the salt gradient from A) and three independent nonlinear pH gradients – black long dashed curve 1^{pH}, red dotted curve 2^{pH} and magenta short dashed curve 3^{pH}. (D) Three DSIGs consisting of the same three step linear salt gradient (dark blue solid line b, the salt gradient from B) and three independent nonlinear pH gradients – black long dashed curve 1^{pH}, red dotted curve 2^{pH}, and magenta short dashed curve 3^{pH}, the same pH gradients as in C. (E) Compositional curves (concentration of solute[1] vs. pH) of the DSDGs shown in panels A and B and DSIGs shown in panel C: thin cyan curve aa^{pH} – DSDGs panel A; thick dashed dark blue curve bb^{pH} – DSDGs panel B; black long dashed curve 1 (a vs. 1^{pH}), red dotted curve 2 (a vs. 2^{pH}) and magenta short dashed curve 3 (a vs. 3^{pH}) for DSIGs from panel C. (Panels F, G and H) Compositional curves of the DSIGs presented in panel D. F – long dashed black curve (b vs. 1^{pH}); G – dotted red curve (b vs. 2^{pH}) and H – short dashed magenta curve (b vs. 3^{pH}). (For interpretation of the references to colour in this figure legend, the reader is referred to the web version of the article.)

as proposed in this theoretical paper. Finally, we will demonstrate that the DSIGs LC does indeed allow systematic scouting and optimization of the separation process (implying that full automation of this process is feasible) to yield significant improvement of the chromatographic selectivity and resolution of proteins' isoforms.

2. Basics of DSIGs

The general scheme for the formation of dual independent gradients of two compounds dissolved in a solvent is fairly straightforward. To execute it requires a quaternary pump LC with four reservoirs, re$_1$–re$_4$ (A–D), a reflection of the fact that development of n independent gradients requires 2^n reservoirs, an assertion we will establish later. The quad LC pump must be able to deliver a well mixed mobile phase stream while pumping at flow rates r_1, r_2, r_3, and $r_4 = r_t - \sum_{n=1}^{3} r_n$ from each of the four reservoirs where r_t is the total flow rate. The individual flows pumped from each of the four reservoirs comprise the four components of the total pumped flow. Thus, if the LC gradient protocol calls for 30% of the flow to originate from reservoir A and the total flow is 1 ml min^{-1}, then the flow from the first reservoir would be $r_1 = 0.3$ ml min^{-1}. The composition of the solutions in each of the four reservoirs must be as follows: reservoir 1 (A) contains the minimum concentration of both MP component one and MP component two, $c_{1,\min}$ and $c_{2,\min}$, reservoir 2 (B) contains the maximum concentration of MP component one, $c_{1,\max}$ and the minimum concentration of MP component two $c_{2,\min}$, reservoir 3 (C) contains the minimum concentration of MP component one $c_{1,\min}$ and the maximum concentration of MP component two $c_{2,\max}$, and reservoir 4 (D) contains the maximum concentration of both solutes, $c_{1,\max}$ and $c_{2,\max}$. Note that any proportionally combined MP from reservoirs 1 and 2 will contain the minimum concentration of MP component 2, but its composition can be adjusted to vary the concentration of MP component 1 arbitrarily between its minimum and maximum concentrations. Likewise, any proportionally combined MP from reservoirs 3 and 4 will contain the maximum concentration of MP component 2, but its composition can also be adjusted to vary the concentration of MP component 1 arbitrarily between its minimum and maximum concentrations. Thus the mathematical description of the flow rates necessary to access any composition in the two dimensional space $[c_1, c_2]$ is characterized by the following partitions if the total flow rate is designated r_t and the flow rate from each reservoir is designated $r_{n,\{n=1-4\}}$:

$$r_1 + r_2 = \frac{c_{2,\max} - c_2}{c_{2,\max} - c_{2,\min}} r_t \quad (1)$$

and

$$r_1 = \frac{c_{1,\max} - c_1}{c_{1,\max} - c_{1,\min}} (r_1 + r_2) \quad (2)$$

$$r_2 = \frac{c_1 - c_{1,\min}}{c_{1,\max} - c_{1,\min}} (r_1 + r_2) \quad (3)$$

$$r_3 + r_4 = \frac{c_2 - c_{2,\min}}{c_{2,\max} - c_{2,\min}} r_t \quad (4)$$

and

$$r_3 = \frac{c_{1,\max} - c_1}{c_{1,\max} - c_{1,\min}} (r_3 + r_4) \quad (5)$$

$$r_4 = \frac{c_1 - c_{1,\min}}{c_{1,\max} - c_{1,\min}} (r_3 + r_4) = r_t - (r_1 + r_2 + r_3) \quad (6)$$

3. Basics of DSIGspH

In the case of a pH gradient and a simultaneous, uncoupled gradient of one non-buffering MP component, the structure of proportioning between the four reservoirs is fundamentally the same as that for DSIGs except that the algebra of proportioning in Eqs.

(1) and (2) is different. This is because, while accurate controlled formation of pH gradients of arbitrary shape over a wide range utilizing pISep buffers is practically achievable, it cannot be accomplished by a simple linear proportional mixing of the acidic and basic pISep buffers over time. To develop pH gradients of defined shape, whether linear or nonlinear, a titration curve of mixtures of the two pISep buffers must be experimentally constructed, represented as percent of the acid pISep buffer ($\%pH_{min}$) as a function of pH. We have found that the titration curve data can be conveniently fitted with high fidelity by a polynomial of order 7–9 in pH [18,19]. For DSIGspH a series of such titration curves, each in the presence of one of a set of systematically varied isocratic concentrations of a non-buffering MP component are experimentally obtained and polynomial equations for each titration curve calculated. From this set of titration curves a mathematical manifold defining a surface in a three dimensional space consisting of ($\%pH_{min}$, pH [MP component, referred to as a solute in the equations below]) can easily be constructed. We have proven in practice that the equation of this manifold can be effectively modeled using a multivariate polynomial as follows:

$$\%pH_{min} = c_n(pH)[solute]^n + c_{n-1}(pH)[solute]^{n-1} + \cdots + c_1(pH)[solute] + c_0 \quad (7)$$

where each $c_n(pH)$ has the form:

$$c_m(pH)^m + c_{m-1}(pH)^{m-1} + \cdots + c_1(pH) + c_0 \quad (8)$$

where n is 3 and m is in the range 7–9 for the DSIGspH manifolds we have constructed. We have calculated these manifolds for three non-buffering compounds, NaCl (0–1 M), urea (0–8 M), and acetonitrile (0–80 vol% and wt%) in the pH range 2.4–10.8.

For the formation of DSIGspH the composition of the buffer solution in each of the four reservoirs must be as follows: reservoir 1 contains pISep buffer at the minimum pH 2.4 ($\%pH_{min}$ = 100) and the minimum concentration of the MP component, $c_{1,min}$; reservoir 2–contains pISep buffer at the minimum pH 2.4 and the maximum concentration of the MP component, $c_{1,max}$;, reservoir 3 contains pISep buffer at the maximum pH 10.8 ($\%pH_{min}$ = 0) and the minimum concentration of the MP component, $c_{1,min}$ and reservoir 4 contains pISep buffer at the maximum pH 10.8 and the maximum concentration of the MP component, $c_{1,max}$. Note that any proportionally combined MP from reservoirs 1 and 2′ will remain at the minimum pH, but its composition can be adjusted to vary the concentration of the additive arbitrarily between its minimum and maximum concentrations. Likewise, any proportionally combined mobile phase from reservoirs 3 and 4 will remain at the maximum pH, but its composition can also be adjusted to vary the concentration of the additive arbitrarily between its minimum and maximum concentrations. Thus to access any composition in the two dimensional space [c_1, pH] the quaternary LC pump has to deliver an MP according to the following partitions if the total flow rate is designated r_t, and the flow rate from each reservoir is designated r_n, $_{\{n=1-4\}}$:

$$r_1 + r_2 = 0.01\%pH_{min} r_t \quad (9)$$

$$r_1 = \frac{c_{1,max} - c_1}{c_{1,max} - c_{1,min}}(r_1 + r_2) \quad (10)$$

$$r_2 = \frac{c_1 - c_{1,min}}{c_{1,max} - c_{1,min}}(r_1 + r_2) \quad (11)$$

$$r_3 + r_4 = 0.01(100 - \%pH_{min})r_t \quad (12)$$

and

$$r_3 = \frac{c_{1,max} - c_1}{c_{1,max} - c_{1,min}}(r_3 + r_4) \quad (13)$$

$$r_4 = \frac{c_1 - c_{1,min}}{c_{1,max} - c_{1,min}}(r_3 + r_4) = r_t - (r_2 + r_3 + r_4) \quad (14)$$

A full analysis and description of algorithms for formation of n multiple independent gradients (MSIGs and MSIGspH), $n \geq 3$ is given in Appendix A where equation numbering continues.

4. Theoretical separations of virtual proteins in DSIGs of pH and salt

4.1. Description of the virtual protein sets

The following theoretical analysis of elution by dual simultaneous independent gradients of salt and pH was performed on a virtual protein set (VPS) whose theoretical elution behavior is derived from the actual elution behavior of ovalbumin (Ova) in a pISep pH gradient separation conducted on a SAX Mono Q column. More explicitly, in a simulated pISep pH gradient with a slope of 0.1 pH unit CV^{-1} (per column volume) beginning at pH 6.6, all of proteins of the VPS would elute at the same apparent pI, pH 4.71, exactly mimicking the observed behavior of the specific Ova isoform in a real pH gradient with the same slope.

Thus, it is important to begin by emphasizing that this analysis is not an attempt to analyze ovalbumin's behavior in particular. Instead we use ovalbumin's elution behavior, its amino acid composition and the electrostatic interaction theory of protein binding to a charged surface [18,19,25–27] to define a set of virtual proteins with very challenging separation properties. These VPs cannot be separated by isoelectric focusing and are difficult to fractionate on an anion exchanger utilizing either a salt gradient at isocratic pH or a pH gradient at isocratic salt concentration. Furthermore, in the paper it will be shown that DSIGs of NaCl and pH on the same SAX SP are theoretically predicted to more successfully overcome the separation challenges posed by this class of proteins than either isoelectric focusing or salt gradients at isocratic pH on the same SP. Actual experimental verification of the increased resolving capability of DSIGspH on various stationary phases has been thoroughly established in numerous experiments in our laboratory and will be published in separate papers.

The fictive ovalbumin congeners are treated here as having no esterified oligosaccharides and thus no sialic acids. Binding free energy is taken as a function of the proteins' charged amino acid residues only. All of the proteins are assumed to contain the same 386 amino acids of ovalbumin with a molecular weight of 42,881 [28], but in this model the proteins can have any primary structure constructible from the ovalbumin amino acid set. The number of distinguishable primary structures for this composition is >2.0e+477. This is so large that we assume that a subset could be found with the desired properties defined here. It is further assumed that each virtual protein will quickly form a folded state in aqueous solution at the usual concentrations encountered in physiological studies. The effective surface area of each of the proteins is set to ~5e+07 m^2 $mole^{-1}$ from the partial molar volume data for ovalbumin [29] and the maximum interacting area is taken to be 1/2 the surface area of the protein. One third of the proteins' residues are taken to be buried leaving 258 residues including all of the ionizable residues on the surface except tyrosine which is taken as effectively buried in this model. Thus, the mean surface area per amino acid is taken to be the effective surface area of the protein divided by 258. With this in mind all of the virtual proteins are assumed to share the same pK_as for each class of surface exposed ionizable residues as follows: aspartate 3.9; glutamate 4.3; histidine 6.08; lysine 10.5; arginine 12; amino terminal 7; and carboxyl terminal 4.0. The pK_as used here are consistent with the reported mean values in proteins [30], but it is obvious that pK_as in actual proteins can vary significantly within each protein for

individual residues of the same class of amino acid and generally from protein to protein. Nevertheless, without losing generality, each residue class can be considered as having one pK_a to reduce unnecessary calculational load. At this point the VPS is of indeterminate size. However it already has the interesting characteristic that all of the proteins would cluster at the same point in a 2D gel electrophoresis separation, whether native or denaturing, because both the mass and the electrophoretic p*I* values are all the same and the assumption of equal surface areas means that we are assuming the hydrodynamic radii are also equal. To further characterize a set of virtual proteins that co-elutes with Ova requires that an expression for the physics of binding of each protein to the stationary phase as a function of protein charge distribution, pH and ionic strength (I) be available, allowing the associated expression for the instantaneous movement of the protein on the stationary phase to be integrated such that the elution can be modeled.

We have recently extended the EI theory of Stahlberg and his colleagues [25–27] using pISep pH gradient chromatography to characterize the general dependence of the retention factor, k, the crucial variable determining the movement of the protein through the column, on both I and pH simultaneously [18,19] (as, defined below). We showed there that a rigorous treatment of the change in a protein's binding free energy as the charge distributions on the protein surface are titrated in response to a pH gradient requires a statistical mechanical analysis and that, in turn, involves an intractable level of calculation even for a known distribution of surface charges. However, the EI equations predict large gains in favorable binding free energy with each positive increment of net opposite charge in a binding region of the protein surface. This lends credence to a model in which one particular charge configuration dominates the binding throughout the pH gradient, and given the aforementioned huge primary sequence space, we consider only a VPS in which the residue composition of the dominant binding charge patch does not vary during elution. Nevertheless, it is important to assert that, in general, for most proteins eluting in a pH gradient, the set of residues dominating the binding free energy should be expected to vary as residues are titrated with changing pH and also as the eluent's I simultaneously varies.

4.2. Retention factor (k) model

These assumptions allow development of a quantitative model for the behavior of the VPS separated under the simultaneous influence of both a pH and a salt gradient. The movement of a protein down into an IEX column is governed by the integral of the inverse of the retention factor, k, which is essentially the fraction of time the protein stays bound to the stationary phase [18,19,25] (the numbering of the following equations continues the numbering of the equations in Appendix A):

$$k(t) = \frac{t_R(t) - t_0}{t_0} \equiv \frac{CV_R(t) - CV_0}{CV_0} \tag{57}$$

$$\int_0^{t_e} \frac{dt}{1+k} = t_0 \equiv \int_0^{CV(t_e)} \frac{dCV}{1+k} = CV_0 \tag{58}$$

$$\ln\ k = \frac{q_p^2}{FA_p(2RT\varepsilon_0\varepsilon_r)^{1/2}\sqrt{I}} + \ln\ \phi \tag{59}$$

$$\phi = \frac{2A_s}{V_0}\left(\frac{\ln 2(RT\varepsilon_o\varepsilon_r)^{3/2}\left(\frac{A_p}{q_p^2} - \frac{1}{A_p\sigma_s^2}\right)}{F(2I)^{1/2}}\right)^{1/2} \tag{60}$$

Here t_0 is the time it takes for a protein to pass through a column without interacting with the stationary phase packed in the column, t_R is the actual retention time of the protein as an instantaneous function of the chemical and physical parameters affecting its binding, i.e. the elution time under conditions of isocratic pH and I equal to those prevailing at a given time, t. Likewise, CV_R is column volume that would be pumped at elution at t_R and CV_0 is column volumes pumped at t_0. They are equivalent under conditions of a constant pumping rate. The actual time until the protein exits the column (is eluted) is t_e and the total pumped column volumes at that time is $CV(t_e)$. The variable q_p is the net charge of that portion of the protein's surface interacting with the stationary phase, A_p is the effective surface area occupied by q_p, I≡I of the buffer solution, F is Faraday's constant, R is the gas constant, T the absolute temperature, ε_0 is the permittivity of the vacuum, ε_r is the dielectric constant of the solution (taken to be that of water since the pISep buffer composition has a very low I). The term $\ln\phi$ is the free energy cost of concentrating the protein in a layer next to the surface of the stationary phase. Here ϕ=(V_l/V_0), a column phase ratio defined as the ratio of the adsorption layer volume, V_l, divided by the sum of the interstitial and pore volumes of an IEX column, V_0. V_l is, in turn, equal to $A_s b$, where A_s is the accessible charged surface area of the stationary phase and b is the thickness of the adsorption layer. A Taylor series expansion of the free energy of analyte distribution in the retention layer as a function of distance from the stationary phase surface is used to estimate b [25]. The term σ_s is the surface charge density of the stationary phase set at 0.3 C m^{-2} (personal communication 2009—Jan Bergström, R&D GE Healthcare).

In Eq. (59) the two terms are formally dimensionless and the first term is in units of ($-\Delta G/RT$) representing the binding free energy of the protein relative to the ambient thermal energy. Thus, k behaves as a normal binding constant with a concentration correction.

The pH dependence of q_p can be made explicit because, if treated as net charge-per-molecule, it can be calculated by using a generalized application of the Henderson–Hasselbalch relation. Each ionizable group has its own unique pK_a. If there are n_i acidic pK_a values and n_j basic pK_a values then for the ith acidic residue having a particular pK_a value:

$$\mathrm{pH} - \mathrm{p}K\mathrm{a}_i = \log_{10}\frac{[Ac_i^-]}{[AcH_i]} \tag{61}$$

and for the jth basic residue having a particular pK_a value:

$$pK_{a_j} - \mathrm{pH} = \log_{10}\frac{[Ba_j^+]}{[Ba_j]} \tag{62}$$

The fractional charge per acidic residue is:

$$q_i = \frac{[Ac_i^-]}{[AcH_i + Ac_i^-]} = \frac{10^{(pH-pK_{a_i})}}{1+10^{(pH-pK_{a_i})}} \tag{63}$$

and the fractional charge per basic residue is

$$q_j = \frac{[Ba_j^+]}{[Ba_j + Ba_j^+]} = \frac{10^{(pK_{a_j}-pH)}}{1+10^{(pK_{a_j}-pH)}} \tag{64}$$

Since in this model all residues of each type charged amino acid have the same pK_a the fractional charge of that group is multiplied by the number of members of the group, m_i or m_j for acidic or basic residue types respectively. With these terms in place an expression for q_p can be constructed:

$$q_p = \sum_i^{n_i} m_i q_i + \sum_j^{n_j} m_j q_j \tag{65}$$

With these tools available the next step in determining the members of the virtual protein set is to analyze the elution behavior of each protein by integrating Eq. (59) in a simulated pISep controlled pH gradient and noting the pH of elution. To define the

binding group the number of each type of ionizable residue in the binding region must be specified as well as the area of interaction. Ovalbumin contains 14 aspartates, 33 glutamates, 7 histidines, 20 lysines, 15 arginines, and, of course, 1 carboxyl terminal and 1 amino terminal. Recall that we already postulated that the 10 tyrosines are regarded for this calculation as buried. The number of distinct groups is then ~5,483,000. The analysis does not suffer loss of generality by considering just one of the four possible end terminal charge configurations as fixed and a minimum of 3 histidines, concessions that reduce the number of distinct groups to ~857,000. For each charge configuration in this reduced set the elution was first simulated with the interaction area set to the maximum, i.e. half the total surface area of the protein, yielding the highest pH of elution for this set of interacting charges because the charge density is thereby minimized. The elution simulation was then repeated with the interaction area set to a close packed array equal to the sum of the individual charged amino acid surface area contributions each taken to be the mean area per amino acid referred to above, yielding the lowest pH of elution because the charge density is then maximized. If the elution pH of the virtual protein fell between these two extremes, the analysis was repeated while systematically stepping to an area value yielding an elution pH (apparent p*I*) within 0.01 pH units of 4.71. That configuration was then added to the VPS. In this way just over 9000 residue configurations were identified that were consistent with the ovalbumin elution pH and the other aforementioned criteria. We reiterate that, because of the way the VPS members were selected, it is easy to see that they would not be separable by 2D GE, either native or denaturing because they have identical molecular weights, identical electrophoretic p*I*'s and identical hydrodynamic radii. Also recall that in a simulated pH gradient commencing at pH 6.6 and descending at 0.1 pH unit CV^{-1}, the entire VPS elutes at pH value 4.71 ± 0.01 pH units. Thus, ordinary pH gradient elution would also completely fail to separate these proteins.

To optimize a virtual salt elution as a control a series of theoretical elutions were run with a very flat salt gradient of 1 mM CV^{-1} at varying isocratic pH values. It was found that for the VPS the optimum pH of binding for salt elution is 5.5 because at higher pH values excessively high salt concentrations, >3 M, were required to elute the most tightly bound proteins.

Three subsets of the VPS were analyzed in detail, a group of 336 virtual proteins, VPSH, with a strong binding to the stationary phase at pH 6.6 (nearly identical large free energy of binding), a second group of 381 virtual proteins, VPSL, with moderate binding to the stationary phase at pH 6.6 (almost identical moderate free energy of binding) and last a third group of 364 proteins, VPSW, calculated to have very weak binding to the stationary phase at pH 6.6 (nearly identical small free energy of binding).

To simulate an actual chromatogram as might be recorded by a UV absorbance detector monitoring the eluent stream, it was assumed that each VP can be detected as a peak with a maximum height of one absorbance unit, each peak is perfectly Gaussian and has a width at half height of one column volume. More explicitly the shape of the peak was assumed to follow a normal equation:

$$A = A_0 \exp[B(x_{\max} - x)^2] \quad (66)$$

where A is the absorbance in relative units, $A_0 = 1$, $B = -\mathrm{Ln}(16)$, x is the number of pumped column volumes and $x_{\max}$ is the CV value at peak maximum. The $x_{\max}$ for each virtual protein was set equal to its calculated elution volume.

Expected absorbance values were calculated at closely spaced pumped CV values from 0 to the elution CV value of the last protein to come off of the column. The values were determined at each CV (x) value by calculating the absorbance contribution of each member of the VPS using Eq. (66) and summing the contributions to give a fictive total absorbance at each pumped column volume value.

4.3. Comparison of virtual separations by salt gradient at Isocratic pH and DSIGs of salt and pH

The gradient profiles of the VPSH optimized separations (virtual chromatograms not shown) by DSIGs of NaCl and pH and the salt gradient at an isocratic pH are shown in Fig. 2 panel A. The single linear step salt gradient (Fig. 2A solid black line 1) ran at 1 mM CV^{-1} from 200 mM NaCl to just under 560 mM NaCl at pH 5.5 (Fig. 2A dashed red line 1^1). The profiles of the two simultaneous decoupled gradients of NaCl and pH are much more complex and somewhat unintuitive (Fig. 2A solid black curve 2 – variable slope salt gradient and solid dark red curve 2^1 variable slope pH gradient). The k values of the virtual proteins of set VPSH are all nearly identical at pH 6.6, but they start to strongly deviate from each other above pH 6.6 and the proteins could be separated by a pH gradient that starts at a much higher pH than pH 6.6 and in the presence of salt. However, if the I were to remain low at that higher pH, then all of the proteins would remain strongly bound to the stationary phase because the induced differences in k would then all be differences between very large numbers. Ergo, the DSIG elution must simultaneously include both a sharply descending pH gradient from alkaline pH 9 and an initially high I (1960 mM NaCl). Subsequently as the pH descends into the range near the proteins' pI, a series of six alternating and synchronously oscillating pH gradients (between pH 5.5 and 6.0 Fig. 2A curve 2^1) and salt (between 200 and 370 mM Fig. 2A curve 2) were developed. It is not obvious but when these gradients are working against each other they are causing gentle changes of the k values that lead to a gradual elution of the VPSH over many column volumes. This competitive strategy was evolved by systematically adding short additional gradient segments characterized by rising pH (stronger protein binding to the SP) and rising salt concentration (weaker protein binding to the SP) working against each other so as to achieve an optimized slow fractionation of the most recalcitrant proteins. A similar approach was used to separate the VPSL (virtual chromatogram – Fig. 2 panel C) by DSIGs of salt and pH (gradient profiles in Fig. 2A: salt gradient – black short dashed curve 4 and pH gradient – dark red dashed curve 4^1). In this case, however it was found that the oscillating gradient strategy is more effective if the competition between pH and I begins after a long isocratic step of salt at 1010 mM over 300 CVs followed by a descending salt gradient between 1010 and 50 mM over 100 CVs coupled to a descending pH gradient from pH 9.3 to pH 5.1.

The binding free energy values for VPSH, the first term in Eq. (59), were checked against the binding free energy values calculated for significantly smaller protein β-lactoglobulin (βlg, MW ~ 18,000) from actual experimental elution data as shown in our earlier paper [18]. At pH 9.7 the binding free energy value for βlg is about 20 RT in 200 mM salt at pH 9.7. For the virtual proteins VPSH it ranges from about 20 to 65 RT at the same pH and salt concentration. Thus, the calculated theoretical values appeared consistent with our earlier published experimental data.

The intrinsic resolution power of the DSIGspH LC in these simulated AEX separations is due to the fact that, at pH values far from the proteins' p*I*s, even closely related iso-forms will often differ significantly in their binding free energy with the stationary phase, meaning that there are very large differences in k. In contrast, such iso-forms tend to have very similar binding energies as the pI is approached. Thus, in AEX elutions the large differences in k would hold at higher alkaline pH values. By utilizing the independence of the gradients to selectively spike the ionic strength in the sections of the gradient wherein pH values are very alkaline, proteins that coelute in salt or, at best, elute only at extremely high salt concentrations, can be pushed to different positions on the column.

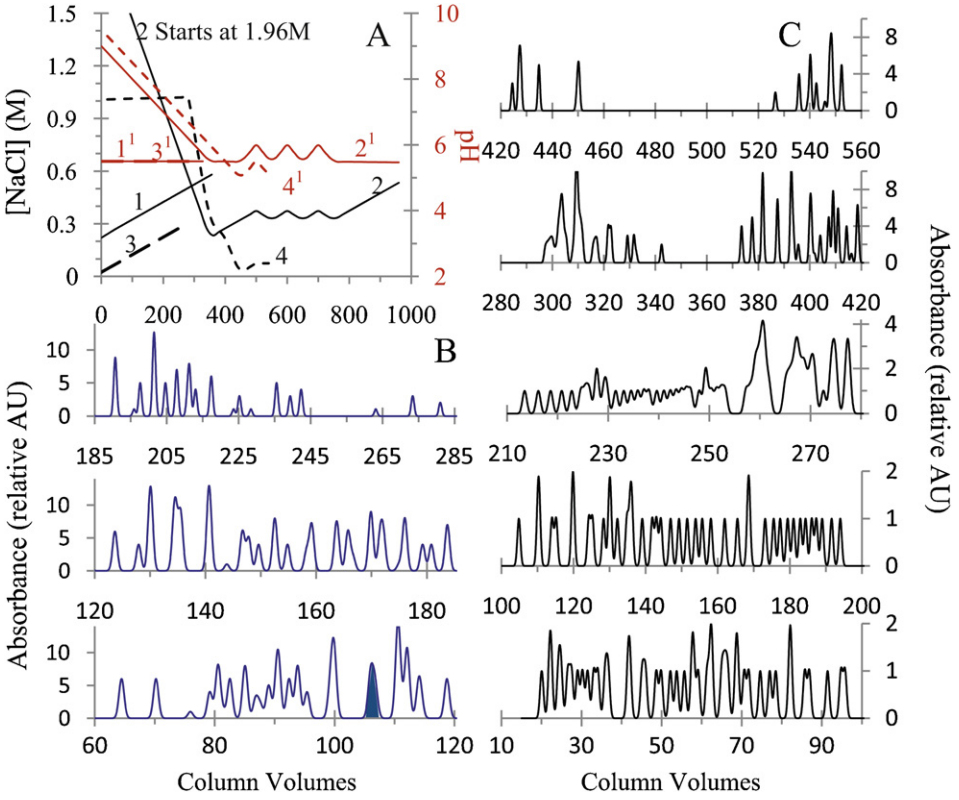

Fig. 2. Gradient profiles used to separate VPSH and VPSL and virtual chromatograms from the separations of VPSL by salt gradient at isocratic pH and DSIGs of salt and pH. Panel A gradient profiles: Solid black line 1 – one step linear salt gradient, 1.0 mM NaCl/CV, from 220 to 600 mM at isocratic pH 5.5 for the separation of VPSH pH represented by the thin solid red horizontal line 1^1. DSIGs for the separation of VPSH consisting of an 8 step nonlinear salt gradient represented by the solid black line 2: step 1 – 4.8 mM NaCl/CV from 1960 to 234 mM, step 2 – 1 mM/CV NaCl from 234 to 372.6 mM, steps 3 to 7 salt gradients oscillating between 372.6 and 333.6 mM with a slope of 1 mM NaCl/CV, step 8 – 1 mM NaCl/CV from 333.6 mM to 534 mM) and simultaneous independent 9 step pH gradient represented by the solid red line 2^1: step 1 – 0.01 pH units/CV from pH 9 to pH 5.5, step 2 – 80 CVs at isocratic pH 5.5, steps 3 – 8 oscillating pH gradients, 0.01 pH units/CV between pH 5.6 and pH 6, step 9 – 220 CVs at isocratic pH 5.5; for the separation of VPSL (chromatogram in panel B) – one step linear salt gradient represented by the long thick dashed black line 3, 1.0 mM NaCl/CV, from 22 to 300 mM at isocratic pH 5.5 the pH represented by the long thick dashed red horizontal line 3^1; DSIG used for the separation of VPSL (chromatogram in panel C) consisting of 5 step nonlinear gradient of salt, represented by the short black dashed curve 4, isocratic step 1 – 280 CVs at 1 M NaCl, step 2 – 8.97 mM NaCl/CV from 1000 to 300 mM NaCl, step 3 – 1.97 mM NaCl/CV from 300 to 260 mM NaCl, step 4 – 2.86 mM NaCl/CV from 260 mM to 35 mM final step 5 – 0.5 mM NaCl/CV from 35 to 75 mM and 4 step independent pH gradient, represented by the short dashed red curve 4^1, step 1 – 0.01 pH units/CV from pH 9.5 to pH 5.1, isocratic step 2 – 20 CVs at pH 5.1, steps 3 and 4 two oscillating pH gradients with slope 0.01 pH units/CV between pH 5.5 and 5.1. (Panel B) Chromatogram from the virtual separation of VPSL using the one step linear salt gradient shown in panel A, lines 1 and 1^1. (Panel C) Chromatogram from the virtual separation of VPSL using DSIGs of salt and pH shown in panel A, curves 4 and 4^1. (For interpretation of the references to colour in this figure legend, the reader is referred to the web version of the article.)

Subsequently the salt concentrations can be reduced while the pH is also reduced to maintain the difference in position as elution proceeds because k values are virtually identical throughout the rest of the elution. Alternatively, keeping the ionic strength at plurality agreement relatively high levels to bring Ln k down to about 7 or less while pH values are varied more or less sinusoidally in the alkaline range will also tend to push difficult to separate species apart on the column and, as in the previous case, because k values are virtually identical throughout the rest of the elution, the proteins will maintain their separation on the column and elute at different times. To demonstrate this a comparison of digital data of four virtual protein congeners from the salt gradient at isocratic pH and the DSIGs of salt and pH for VPSH is detailed in Table 1.

The chromatographic resolution quality is based on the deconvolution analysis of the chromatograms of the VPSH (virtual chromatograms not shown), VPSL separations by salt gradient at isocratic pH (virtual chromatogram Fig. 2 panel B), and DSIGs of salt and pH (virtual chromatogram Fig. 2 panel C). It is illustrated and compared in Fig. 3. In each VPSH and VPSL separation chromatogram the number of individual proteins responsible for at least 90% of the area under each chromatographic peak was calculated. The width at base (CVs) of each peak was taken to be from the nearest absorbance minimum before the peak maximum to the nearest minimum following the peak maximum. The results from the deconvolution chromatographic analysis show that in the salt gradient separation at isocratic pH the 336 proteins of VPSH are eluted in 24 peaks averaging about 14 proteins per peak (Fig. 3A). One peak contains 9 proteins and all other peaks contain 10 or more up to 29 proteins per peak. This would be a good separation for proteomics and a useful pre-purification step, but none of the proteins is close to being pure. In comparison, the deconvolution analysis of the significantly better resolved proteins of the VPSH (336 proteins were eluted in 70 peaks Fig. 3B) in the DSIGs of salt and pH separation estimates that 38.57%, or 27 of the 70 virtually separated peaks contain completely purified protein and another 31.43%, or 22 of the 70 peaks contain 2–4 proteins each. The remaining 21 peaks on average contain about 13 proteins per peak, which is a modest improvement over salt elution at isocratic pH. A comparison of the deconvolution chromatographic analyses of the VPSL separations utilizing salt at isocratic pH (Fig. 3C – virtual chromatogram shown in Fig. 2B) vs. DSIGs salt and pH (Fig. 3D – virtual chromatogram shown in Fig. 2C) reveals as for VPSH a strong resolution improvement in the virtual dual gradient separation. Here the average chromatographic peak in the salt gradient separation at isocratic pH contains on average 7.25 proteins while the average peak in the DSIGs of salt and pH contains on average 3.33 proteins.

Table 1
Virtual AEX LC digital elution data for four virtual protein congeners chosen from the virtual protein set VPSH. The virtual proteins differ in the composition of the charged amino acids forming each binding surface patch, but the binding patch area interacting with the stationary phase is virtually identical. While the four proteins co-elute in a salt gradient at isocratic pH 5.5 they are well resolved by a dual simultaneous gradient of pH and NaCl (both gradient protocols are described in the caption of Fig. 2A). Abbreviations: (1) names of the charged amino acids: lysine – Lys; arginine – Arg; histidine – His; glutamic acid – Glu; aspartic acid – Asp; (2) column volumes: CVs.

Charged amino acid composition and area of the binding patches of 4 VPSH						Virtual separation of 4 VPSH by salt gradient at pH 5.5				Virtual separation of 4 VPSH by DSIGs of NaCl and pH			
Lys	Arg	His	Glu	Asp	Area (m^2/mole of protein)	pH	[NaCl] (mM)	Ln k	Elution CVs	pH	[NaCl] (mM)	Ln k	Elution CVs
1	15	4	16	13	24782753.459	5.500	277.1395	3.545	53.248	8.658	1785.993	3.732	35.185
2	14	4	16	13	24782784.163	5.500	277.1395	3.545	53.248	8.647	1780.365	3.763	36.323
13	3	4	16	13	24783121.540	5.500	277.1395	3.545	53.252	8.506	1710.604	4.070	50.421
14	2	4	16	13	24783152.157	5.500	277.1395	3.545	53.253	8.492	1703.614	4.096	51.833

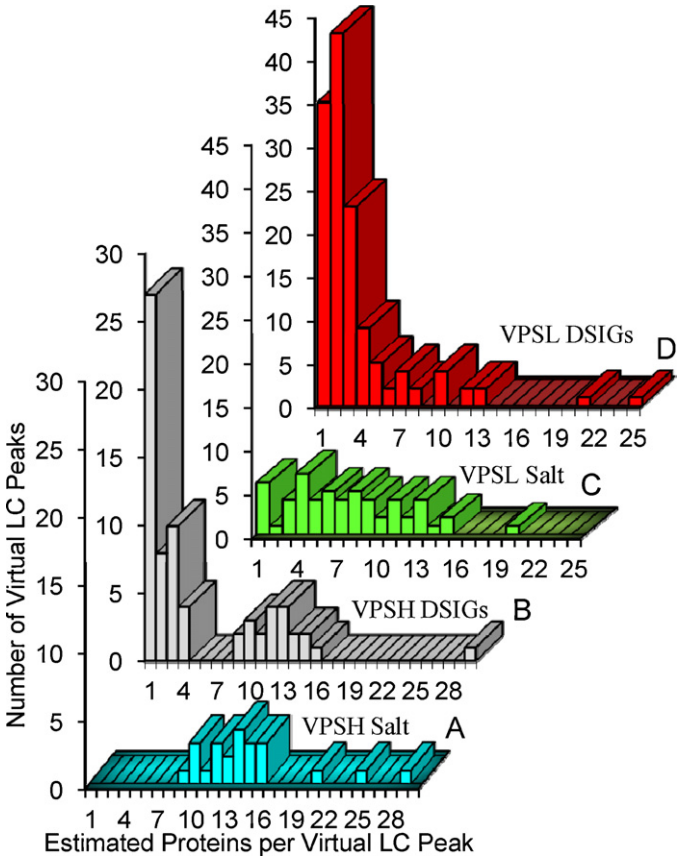

Fig. 3. Comparison of a salt gradient at isocratic pH and DSIGs of salt and pH theoretical separations of VPSH (panels A and B) and VPSL (panels C and D). The resolution quality of the separations is evaluated by bar plots presenting the number of virtually detected chromatographic peaks (y axis) versus the number of estimated proteins per chromatographic peak (x axis). The number of proteins per peak is estimated by deconvolution analyses of the virtually detected chromatographic peaks and is the number of proteins accounting for at least 90% of the area under the peak being analyzed. (For interpretation of the references to colour in this figure legend, the reader is referred to the web version of the article.)

In salt 10.7%, 6 of the 56 virtual peaks consist of entirely purified protein while 21.4%, 12 of the 56 peaks contain 2–4 proteins per peak. The resolution improvement in the DSIGs of salt and pH separation is again very significant where 26.3%, or 35 of the 133 peaks contain fully purified protein and another 56.4%, 75 of the 133 peaks contain 2–4 virtual proteins.

Fig. 4 illustrates the gradient profiles used to virtually separate the very low binding affinity VPSW by salt gradient at isocratic pH (solid black line 1 and – short dashed black horizontal line 1^1) and two DSIGs of salt and pH (DSIGs 1: salt gradient – thick solid red line 2 and independent pH gradient – dotted red curve 2^1; DSIGs 2: salt gradient – dash dotted blue curve 3 and independent pH gradient – solid blue curve 3^1). By taking advantage of the strong binding at high pH of these otherwise weak binding proteins at pH 6.6, the simulated virtual elution by a linear salt gradient yields an excellent separation at high salt, and alkaline pH 9 (virtual chromatograms not shown). The 364 virtual proteins of the VPSW are fractionated in 251 observable peaks or 1.45 proteins per peak. 77% of the proteins are eluted in the salt concentration range 300–1000 mM, and the other 23% in the range 1000–1900 mM. The first DSIGs protocol (Fig. 4 salt gradient curve 2 and pH gradient dashed curve 2^2) also separates the VPSW in 251 peaks or 1.45 proteins per peak. A total of 74.9% of the proteins were eluted between 100 and 740 mM NaCl and at pH values oscillating between 8 and 9. The rest of the proteins were eluted between 740 and 1070 mM NaCl and in a descending

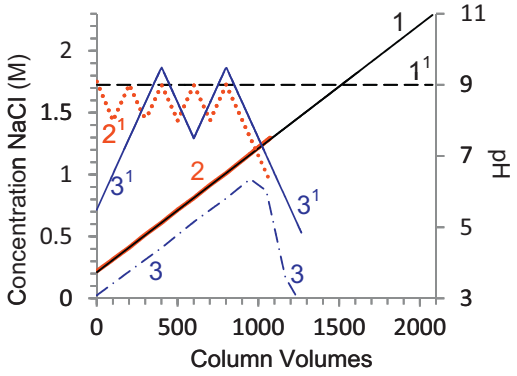

Fig. 4. Profiles of a salt gradient at isocratic pH and two DSIGs of salt and pH used to virtually separate VPSW. Black solid line 1 – one step linear salt gradient, 1.1 mM NaCl/CV from 210 to 2289 mM NaCl, at isocratic pH 9 represented by the dashed black horizontal line 1^1. First DSIGs of salt and pH: thicker solid red line 2 – salt gradient, 1.2 mM NaCl/CV from 220 to 1295 mM NaCl and dotted red line 2^1 the independent pH gradient starting with eight pH gradient steps oscillating between pH 8 and pH 9 with slope 0.01 pH units/CV over 560 CVs, and a final 9th step, 0.01 pH units/CV from pH 9 to pH 6.3. Second DSIGs of salt and pH: dash-dotted blue line 3 – five step salt gradient, step 1, 0.99 mM NaCl/CV from 0 to 964 mM NaCl; step 2, 0.96 mM/CV from 964 to 869 mM; step 3, 5.96 mM NaCl/CV from 869 to 171 mM NaCl; step 4, 2.2 mM NaCl/CV from 171 to 24.5 mM NaCl, and a final isocratic step 5, 34 CVs at 24.5 mM NaCl, and an independent 4 step nonlinear pH gradient represented by the solid blue line 3^1, – segment 1, 0.01 pH units/CV from pH 5.5 to pH 9.4; segments 2 and 3, two pH gradients oscillating between pH 9.4 and pH 7.5 with slope 0.01 pH units/CV; and a final segment 4, 0.0096 pH units/CV from pH 9.4 to pH 4.85. (For interpretation of the references to colour in this figure legend, the reader is referred to the web version of the article.)

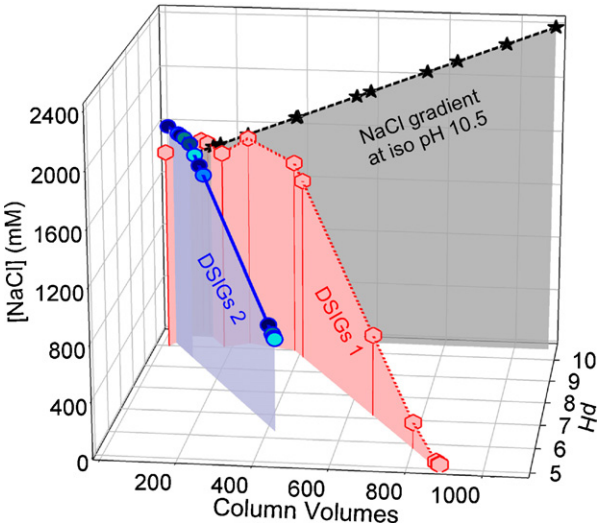

Fig. 5. Repeat virtual AEX LC of 12 co-eluting VPSL in the peak eluting at 106 column volumes as shown in Fig. 2 panel B. Comparison of separations by an optimized salt gradient at isocratic pH with two DSIGs of pH and salt. The 12 proteins separated by a salt gradient at isocratic pH 10.5 represented by the black filled stars, 1 mM NaCl/CV from 1300 mM to 2400 mM. Black dashed line – compositional curve of the gradient ([NaCl] vs. pH). The 12 proteins separated by DSIGs protocol #1 represented by Red line rose filled hexagons. Red dotted curve – compositional curve of DSIGs #1: salt gradient – step 1, 200 CVs isocratic at 1450 mM NaCl; step 2, 2 mM NaCl/CV 1450 mM to 1650 mM; step 3, 3 mM NaCl/CV 1650 to 24.5 mM; step 4, 30 CVs isocratic at 24.5 mM salt and 4 step independent pH gradient – steps 1–3, 300 CVs pH gradients ascending–descending–ascending between pH 10 and pH 10.8 at 0.01pH units/CV; step 4, 0.01 pH units from pH 10.8 to pH 4.9. The 12 proteins separated by DSIGs #2 represented by the blue line with blue filled circles of variable hue. Blue solid curve – compositional curve of DSIGs #2: two step salt gradient – step 1, 100 CVs isocratic at 1600 mM NaCl; step 2, 3 mM NaCl/CV 1600 mM to 650 mM and one step independent pH gradient, 0.01 pH units/CV from pH 10.3 to pH 6.3. Remark – due to the angle of rotation not all of the 12 separated proteins can be seen well in all of the 3D plots. (For interpretation of the references to colour in this figure legend, the reader is referred to the web version of the article.)

pH gradient from pH 9 to pH 6.2. The second DSIGs protocol (Fig. 4 salt gradient solid blue curve 3 and pH gradient dashed blue curve 3^1) separates the VPSW into 246 peaks or 1.48 proteins per peak. Here 54.9% of the proteins were eluted between 100 and 780 mM NaCl and at pH values oscillating between 9 and 6. The other 49.1% of the proteins were eluted between 780 and 1270 mM NaCl and in a descending pH gradient from pH 9 to pH 4.8. Although the two DSIGs protocols did not improve the resolution of the salt gradient separation at isocratic pH of the VPSW they reduce substantially the separation time and demonstrate the flexibility of this new gradient LC technique enabling the chromatographer to scout and change in a controlled manner proteins' separation conditions such as the elution pH and concentration of salt.

In Fig. 5 we examine, how well either secondary DSIGs of salt and pH or a secondary salt gradient at an alkaline isocratic pH can resolve a small subset of unresolved proteins from the VPSL during their primary salt gradient separation. The analyzed protein subset is virtually eluted in the dark blue filled peak at 106 CVs shown in the virtual chromatogram, Fig. 2 panel B. It was eluted by the salt gradient at isocratic pH having the profile shown in Fig. 2 panel A – black line 1 (slope 1 mM NaCl/CV 0–380 mM) and red thin solid horizontal line1^1 (isocratic pH 5.5). The deconvolution analysis estimates the presence of 12 unresolved proteins in this baseline resolved peak that can be grouped into four intimately related sets based on the congruence of the number of charged residues of aspartic and glutamic acid, arginine, lysine and histidine in their binding site amino acid composition. Two of the groups consist of only one protein. The first monotypic set has: 7 Asp, 6 Glu, 3 His, 5 Arg and no Lys and the second: 6 Asp, 4 Glu, 3 His, 3 Arg and no Lys. The last two sets contain four and six proteins respectively. Within each set they differ only in the number of arginine and lysine residues in the binding region, where the sum of arginines and lysines is also constant within each set. Set 3: protein 3-1 – 11 Asp, 6 Glu, 6 His, 5 Arg and no Lys; protein 3-2 – 11 Asp, 6 Glu, 6 His, 4 Arg and 1 Lys; protein 3-3 – 11 Asp, 6 Glu, 6 His, 3 Arg and 2 Lys; protein 3-4 – 11 Asp, 6 Glu, 6 His, 2 Arg and 3 Lys; protein 3-5 – 11 Asp, 6 Glu, 6 His, 1 Arg and 4 Lys; protein 3-6 – 11 Asp, 6 Glu, 6 His, 0 Arg and 5 Lys. Step 4: protein 4-1 – 10 Asp, 4 Glu, 6 His, 3 Arg and no Lys; protein 4-2 – 10 Asp, 4 Glu, 6 His, 2 Arg and 1 Lys; protein 4-3 – 10 Asp, 4 Glu, 6 His, 1 Arg and 2 Lys; protein 4-4 – 10 Asp, 4 Glu, 6 His, 0 Arg and 3 Lys. As a result of these binding site structural limitations, the only pH range in which the *k* values of the members of each group differ significantly from each other is in the pH range circa the pK_a values of the arginine and lysine residues (9.5–12). After an intensive virtual scouting of the gradient elution conditions it was found that a salt gradient with a slope of 1 mM/CV at high salt concentration from 1300 to 2400 mM and at high alkaline isocratic pH 10.5 (gradient compositional line shown in Fig. 5 black dashed line) can completely separate the 12 proteins (Fig. 5 black filled stars) of the virtual sample in 1100 CVs. It was found that many DSIGs of salt and pH (the compositional profiles for two DSIGs are shown in Fig. 5 – the blue solid curve and the red dotted curve) are also capable of completely separating the 12 proteins (Fig. 5, red line rose filled hexagons and blue solid curve with blue filled circles) of variable hue but at the same time providing substantial advantages over the separation by salt gradient at isocratic pH. These include lowering the elution pH and salt concentration ranges for some of the proteins as well as reducing the chromatography run time (fewer column volumes). One of the DSIGs elutes the 12 VPSL proteins in the pH range from pH 10.5 to pH 5.5 and salt concentrations from 1500 mM to 140 mM (Fig. 5 red line rose filed hexagons and red dotted curve). The second DSIG fractionates the twelve proteins in the pH range from pH 10.3 to pH 6.3 and salt concentrations from 1600 mM to 650 mM (Fig. 5 blue solid curve with blue line blue filled circles of variable hue). The

run time of separation is substantially reduced from 1100 CVs in salt at isocratic pH to 880 CVs and 425 CVs respectively for the two DSIGspH protocols. That is 1.25 and 2.5 times faster separation by the DSIGs (Fig. 5).

5. Conclusions

In this paper we describe mathematically rigorous algorithms for creating simultaneous independent LC gradients of n solutes where $n \geq 2$ and simultaneous independent LC gradients of pH and n solutes where $n \geq 1$. We also theoretically explore and compare the application of DSIGspH gradients vs. that of salt gradients at isocratic pH to the fractionation of virtual protein mixtures inseparable by either isoelectric focusing or SDS page gel electrophoresis. It is concluded that DSIGspH improves IEX chromatographic resolution, decreases separation time, and allows independent scouting and more flexible adjustment of elution conditions when compared to traditional salt gradients at isocratic pH. pISep chromatography with dual simultaneous, independent gradients of pH and salt or pH and organic solvents such as acetonitrile makes it possible to conduct the traditional two step consecutive one dimensional chromatography (isoelectric focusing, chromatofocusing or IEX followed by reversed phase) as a one step two dimensional liquid chromatography for proteins separations.

5.1. Algorithms

In our 2008 paper [18] describing the precise control of pH gradients in the absence of salt we said: "We have shown that the mixing of the pISep basic and the pISep acidic buffers can be algorithmically calculated with sufficient accuracy using a high order polynomial fit to the pISep titration curve to accurately generate multi-step, multi-slope, linear, nonlinear or combined linear and nonlinear pH gradients on a wide range of weak and strong AEX and CEX stationary phases." Here we have shown: (1) how to uncouple simultaneous gradients of two or more MP components; and (2) how to uncouple mathematically characterized pH gradients such as those developed by pISep from simultaneous gradients of one or more non-buffering MP components. We have provided a theoretical framework for understanding why DSIGs should improve chromatographic resolution compared to that of single component gradients, i.e. the retention factor, k is proportional to the exponent of the sum of independent binding free energies.

5.2. Theoretical elutions

Using the EI theory of protein binding to charged stationary phases, the primary structure and the elution behavior of avian ovalbumin in a descending pISep pH gradient on an AEX SP, we constructed a virtual protein set that eluted at the same pH as Ova and had calculated binding energies consistent with measured values for βlg [18]. This VPS had the interesting property of not only emerging at the same apparent pI in a pISep pH gradient, but also being inseparable by 2D gel electrophoresis (isoelectric focusing followed by SDS page). Virtual elutions by DSIGspH and salt gradients at constant pH were optimized for the separation of selected subsets of the VPS possessing varying strengths of binding. Comparison of the optimized virtual fractionations established a series of advantages of DSIGspH over salt gradient elutions at isocratic pH. At intermediate and high binding free energies a significantly higher proportion of proteins could actually be purified from complex mixtures by DSIGspH when compared to salt. In lightly bound proteins or small groups of proteins that co-elute, both salt and DSIGspH could successfully purify the target proteins, but in DSIGspH the purification could be optimized over different pH ranges and often at much lower salt concentrations and shorter run times.

Acknowledgements

The authors wish to acknowledge the support of the Director of the Biomedical Research Institute, Dr James Leef, and the Board of Directors of the American Foundation for Biological Research. Critical editing by the late Dr Harold Meryman was invaluable. Valuable support during this research was provided by Jeff Conroy of Adjuvant, LLC. Dr V Adrian Parsegian of the U of Mass provided important advice on the physics of protein interaction with charged surfaces. Jordan Hirsh offered helpful mathematical comments.

Appendix A. Basics of MSIGs and MSIGspH for three independent gradients

Examination of the description of the reservoirs' contents in the examples above and Eqs. (1)–(6) and (9)–(14) provide an explanation of why 2^n reservoirs are necessary for n simultaneous independent gradients. For each of the n components the solutions in half of the reservoirs must contain the MP component at its maximum concentration (or be at the maximum pH value) and in the other half of the reservoirs the solutions must contain the MP component at its minimum concentration (or be at the minimum pH value). Additionally, within the mth such subgroup ($m \leq (n-1)$) all of the reservoirs must form further subgroups such that in each such subgroup half of the reservoirs contain either the maximum or the minimum concentration of every one of the remaining n–m components. Thus, to accomplish three independent gradients requires 8 reservoirs because $2^3 = 8$, and the composition of the fluid in each reservoir is as follows: reservoir 1 contains the minimum concentration of all three components, $c_{1,\min}$, $c_{2,\min}$, $c_{3,\min}$, reservoir 2 contains $c_{1,\max}$, $c_{2,\min}$, $c_{3,\min}$, reservoir 3 contains $c_{1,\min}$, $c_{2,\max}$, $c_{,\min}$, reservoir 4 contains $c_{1,\max}$, $c_{2,\max}$, $c_{3,\min}$, reservoir 5 contains $c_{1,\min}$, $c_{2,\min}$, $c_{3,\max}$, reservoir 6 contains $c_{1,\max}$, $c_{2,\min}$, $c_{3,\max}$, reservoir 7 contains $c_{1,\min}$, $c_{2,\max}$, $c_{3,\max}$, reservoir 8 contains all three components at their maximum concentration $c_{1,\max}$, $c_{2,\max}$, and $c_{3,\max}$.

Flows from reservoir 1 through reservoir 4 are isocratic in c_3 at its minimum. Note that any combined MP from reservoirs 1 and 2 will contain the minimum concentration of both components 2 and 3, but its composition can be adjusted to vary the concentration of MP component 1 arbitrarily between its minimum and maximum concentrations. Likewise, any combined MP from reservoirs 3 and 4 will contain the maximum concentration of MP component 2 and the minimum concentration of MP component 3, but its composition can also be adjusted to vary the concentration of MP component 1 arbitrarily between its minimum and maximum concentrations and in particular to match the concentration of MP component 1 in the MP stream from reservoirs 1 and 2. The combined flows from reservoirs 1 + 2 and reservoirs 3 + 4 can then be adjusted with respect to each other to provide in the mobile phase any concentration of MP component 2 between its maximum and minimum values without effecting the concentration of the other solutes because they are isocratic within this group of mixed flows. This description is repeated for flows from reservoirs 5–8 that are all isocratic in c_3 at its maximum. To access any composition in the three dimensional space [c_1–c_3] mobile phase is pumped according to the following mathematical partition algorithms with the total flow rate designated by r_t and the flow rate from each reservoir designated by r_n, $_{\{n=1-8\}}$:

$$r_1 + r_2 + r_3 + r_4 = \frac{c_{3,\max} - c_3}{c_{3,\max} - c_{3,\min}} r_t \tag{15}$$

and

$$r_1 + r_2 = \frac{c_{2,\max} - c_2}{c_{2,\max} - c_{2,\min}}(r_1 + r_2 + r_3 + r_4) \quad (16)$$

$$r_1 = \frac{c_{1,\max} - c_1}{c_{1,\max} - c_{1,\min}}(r_1 + r_2) \quad (17)$$

$$r_2 = \frac{c_1 - c_{1,\min}}{c_{1,\max} - c_{1,\min}}(r_1 + r_2) \quad (18)$$

$$r_3 + r_4 = \frac{c_2 - c_{2,\min}}{c_{2,\max} - c_{2,\min}}(r_1 + r_2 + r_3 + r_4) \quad (19)$$

and

$$r_3 = \frac{c_{1,\max} - c_1}{c_{1,\max} - c_{1,\min}}(r_3 + r_4) \quad (20)$$

$$r_4 = \frac{c_1 - c_{1,\min}}{c_{1,\max} - c_{1,\min}}(r_3 + r_4) \quad (21)$$

$$r_5 + r_6 + r_7 + r_8 = \frac{c_3 - c_{3,\min}}{c_{3,\max} - c_{3,\min}} r_t \quad (22)$$

and

$$r_5 + r_6 = \frac{c_{2,\max} - c_2}{c_{2,\max} - c_{2,\min}}(r_5 + r_6 + r_7 + r_8) \quad (23)$$

$$r_5 = \frac{c_{1,\max} - c_1}{c_{1,\max} - c_{1,\min}}(r_5 + r_6) \quad (24)$$

$$r_6 = \frac{c_1 - c_{1,\min}}{c_{1,\max} - c_{1,\min}}(r_5 + r_6) \quad (25)$$

$$r_7 + r_8 = \frac{c_2 - c_{2,\min}}{c_{2,\max} - c_{2,\min}}(r_5 + r_6 + r_7 + r_8) \quad (26)$$

and

$$r_7 = \frac{c_{1,\max} - c_1}{c_{1,\max} - c_{1,\min}}(r_7 + r_8) \quad (27)$$

$$r_8 = \frac{c_1 - c_{1,\min}}{c_{1,\max} - c_{1,\min}}(r_7 + r_8) \quad (28)$$

For MSIGspH with two MP components (referred to as solutes in all the equations below) the manifold equations defining $\%\mathrm{pH}_{\min}$ are more elaborate than those for DSIGspH. The relevant equation represents a three dimensional manifold of pH and two solutes:

$$\begin{aligned}\%\mathrm{pH}_{\min} = {} & C_{n_1}(\mathrm{pH}, \mathrm{solute}_2) \\ & \times [\mathrm{solute}_1]^{n_1} + C_{n_1-1}(\mathrm{pH}, \mathrm{solute}_2)[\mathrm{solute}_1]^{n_1-1} \\ & + \cdots + C_1(\mathrm{pH}, \mathrm{solute}_2)[\mathrm{solute}_1] + C_0(\mathrm{pH}, \mathrm{solute}_2)\end{aligned} \quad (29)$$

where each $C_k(\mathrm{pH},\mathrm{solute}_2)$, $k = 0$ to n_1 has the form:

$$C_{n_2}(\mathrm{solute}_2)\mathrm{pH}^{n_2} + C_{n_2-1}(\mathrm{solute}_2)\mathrm{pH}^{n_2-1} + \cdots + C_1(\mathrm{solute}_2)\mathrm{pH} + C_0(\mathrm{solute}_2) \quad (30)$$

and each $C_m(\mathrm{solute}_2)$, where $m = 0$ to n_2 has the form:

$$C_{m,j}\mathrm{solute}_2^j + C_{m,j-1}\mathrm{solute}_2^{j-1} + \cdots + C_{m,1}\mathrm{solute}_2 + C_{m,0}, j \quad \text{usually} = 3 \quad (31)$$

where the full set of $c_{m,j}$ are fitting constants.

To access any composition in the three dimensional space [c_1, c_2, pH] eluent is pumped according to the following partitions with the total flow rate designated by r_t and the flow rate from each reservoir designated by r_n, $_{\{n=1-8\}}$:

$$r_1 + r_2 + r_3 + r_4 = 0.01\%pH_{\min} r_t \quad (32)$$

and

$$r_1 + r_2 = \frac{c_{2,\max} - c_2}{c_{2,\max} - c_{2,\min}}(r_1 + r_2 + r_4 + r_4) \quad (33)$$

$$r_1 = \frac{c_{1,\max} - c_1}{c_{1,\max} - c_{1,\min}}(r_1 + r_2) \quad (34)$$

$$r_2 = \frac{c_1 - c_{1,\min}}{c_{1,\max} - c_{1,\min}}(r_1 + r_2) \quad (35)$$

$$r_3 + r_4 = \frac{c_2 - c_{2,\min}}{c_{2,\max} - c_{2,\min}}(r_1 + r_2 + r_3 + r_4) \quad (36)$$

and

$$r_3 = \frac{c_{1,\max} - c_1}{c_{1,\max} - c_{1,\min}}(r_3 + r_4) \quad (37)$$

$$r_4 = \frac{c_1 - c_{1,\min}}{c_{1,\max} - c_{1,\min}}(r_3 + r_4) \quad (38)$$

$$r_5 + r_6 + r_7 + r_8 = 0.01(100 - \%\mathrm{pH}_{\min})r_t \quad (39)$$

and

$$r_5 + r_6 = \frac{c_{2,\max} - c_2}{c_{2,\max} - c_{2,\min}}(r_5 + r_6 + r_7 + r_8) \quad (40)$$

$$r_5 = \frac{c_{1,\max} - c_1}{c_{1,\max} - c_{1,\min}}(r_5 + r_6) \quad (41)$$

$$r_6 = \frac{c_1 - c_{1,\min}}{c_{1,\max} - c_{1,\min}}(r_5 + r_6) \quad (42)$$

$$r_7 + r_8 = \frac{c_2 - c_{2,\min}}{c_{2,\max} - c_{2,\min}}(r_5 + r_6 + r_7 + r_8) \quad (43)$$

and

$$r_7 = \frac{c_{1,\max} - c_1}{c_{1,\max} - c_{1,\min}}(r_7 + r_8) \quad (44)$$

$$r_8 = \frac{c_1 - c_{1,\min}}{c_{1,\max} - c_{1,\min}}(r_7 + r_8) \quad (45)$$

A.1. The general flow equations for MSIGs and MSIGspH

We develop a formal description of the distribution of n additives among 2^n reservoirs. Consider the mth reservoir. If m is even then the first additive is at its maximum, if m is odd the first additive is at its minimum. This is equivalent to saying that if $(m \bmod 2^1) = 0$ then $c_{1,m} = c_{1,\max}$, else $c_{1,m} = c_{1,\min}$. Continuing, if $(m \bmod 2^2) > 2^1$ or $(m \bmod 2^2) = 0$ then $c_{2,m} = c_{2,\max}$, else $c_{2,m} = c_{2,\min}$. This pattern is generalized as: if $(m \bmod 2^k) > 2^{k-1}$ or $(m \bmod 2^k) = 0$ then,

$$c_{k,m} = c_{k,\max}, \text{ else } c_{k,m} = c_{k,\min} \text{ for } k = 1, 2, \ldots, n \quad (46)$$

This leads to an equally compact expression for r_m. Clearly, if $c_{k,m} = c_{k,\max}$, then the coefficient multiplying r_t for this additive is $Coefficient(c_{k,m}) = (c_k - c_{k,\min})/c_{k,\max} - c_{k,\min}$, and, conversely, if $c_{k,m} = c_{k,\min}$, then the coefficient multiplying r_t for this additive is $\text{coefficient}(c_{k,m}) = (c_{k,\max} - c_k)/c_{k,\max} - c_{k,\min}$. The general equation is then:

$$r_m = \Pi_{k=1}^{n}\ Coefficient(c_{k,m}) r_t \quad (47)$$

As an example, suppose $n = 3$, $m = 5$, i.e. the 5th reservoir in a three additive system. Then the flow rate demanded from the fifth reservoir, r_5, when the gradient protocol calls for solutes concentrations c_1, c_2, and c_3, is calculated as follows. Since 5 is odd, $c_{1,5} = c_{1,\min}$. Then, since $(5 \bmod 2^2) = 1 \leq 2$, $c_{2,5} = c_{2,\min}$. Then, since for additive 3, $(5 \bmod 2^3) > 2^2$, $c_{3,5} = c_{3,\max}$. From this we write the flow rate equation immediately as:

$$r_5 = \frac{c_{1,\max} - c_1}{c_{1,\max} - c_{1,\min}} \frac{c_{2,\max} - c_2}{c_{2,\max} - c_{2,\min}} \frac{c_2 - c_{2,\min}}{c_{2,\max} - c_{2,\min}} r_t$$

Thus, this yields a single flow rate equation for each reservoir.

In the case of MSIGspH all of the above is unchanged except that there are $n - 1$ additives so k goes from 1 to $n - 1$. The expression

for determining the pH value of the mth reservoir is as follows: if $(m \bmod 2^n) > 2^{n-1}$ or $(m \bmod 2^n) = 0$

$$\text{then } \mathrm{pH}(m) = \mathrm{pH}_{\max}, \quad \text{else}, \quad \mathrm{pH}(m) = \mathrm{pH}_{\min} \tag{48}$$

then the flow rate equations are:

$$r_m = \Pi_{k=1}^{n-1} \mathit{Coefficient}\,(c_{k,m}) 0.01\%\mathrm{pH}_{\min} r_t \quad \text{for } \mathrm{pH}(m) = \mathrm{pH}_{\min} \tag{49}$$

and

$$r_m = \Pi_{k=1}^{n-1} \mathit{Coefficient}(c_{k,m}) 0.01(100 - \%\mathrm{pH}_{\min}) r_t \quad \text{for } \mathrm{pH}(m) = \mathrm{pH}_{\max} \tag{50}$$

where $\mathit{Coefficient}(c_{k,m})$ is defined as previously for each of the $n-1$ additives.

The $\%\mathrm{pH}_{\min}$ equation must be generalized as well and for $n \geq 4$ this presents real practical impediments because the number of fitting constants grows exponentially with the number of additives. Explicitly we have for $n-1$ additives plus pH, expanding from Eqs. (29)–(31):

$$\begin{aligned}\%\mathrm{pH}_{\min} = {} & c_{n_1}(\mathrm{pH}, \mathrm{solute}_{n-1}, \mathrm{solute}_{n-2}.....\mathrm{solute}_2)[\mathrm{solute}_1]^{n_1} \\ & + c_{n_1-1}(\mathrm{pH}, \mathrm{solute}_{n-1}, \mathrm{solute}_{n-2}, \ldots, \mathrm{solute}_2) \\ & [\mathrm{solute}_1]^{n_1-1} + \cdots + c_1(\mathrm{pH}, \mathrm{solute}_{n-1}, \mathrm{solute}_{n-2}, \ldots, \\ & \mathrm{solute}_2)[\mathrm{solute}_1] + c_0(\mathrm{pH}, \mathrm{solute}_{n-1}, \mathrm{solute}_{n-2}, \\ & \ldots, \mathrm{solute}_2)\end{aligned} \tag{51}$$

where each $c_k(\mathrm{pH}, \mathrm{solute}_{n-1}, \mathrm{solute}_{n-2}, \ldots, \mathrm{solute}_2)$, $k = 0$ to n_1 has the form:

$$\begin{aligned}& c_m(\mathrm{solute}_{n-1}, \mathrm{solute}_{n-2}, \ldots, \mathrm{solute}_2)\mathrm{pH}^m + c_{m-1}(\mathrm{solute}_{n-1}, \\ & \mathrm{solute}_{n-2}, \ldots, \mathrm{solute}_2)\mathrm{pH}^{m-1} + \cdots + c_1(\mathrm{solute}_{n-1}, \mathrm{solute}_{n-2}, \\ & \ldots, \mathrm{solute}_2)\mathrm{pH} + c_0(\mathrm{solute}_{n-1}, \mathrm{solute}_{n-2}, \ldots, \mathrm{solute}_2) \\ & m \text{ usually} > 6 \text{ for the pISep buffers}\end{aligned} \tag{52}$$

And, in turn, each $c_m(\mathrm{solute}_{n-1}, \mathrm{solute}_{n-2}, \ldots, \mathrm{solute}_2)$ has the form:

$$\begin{aligned}& c_{n_2}(\mathrm{solute}_{n-1}, \mathrm{solute}_{n-2}, \ldots, \mathrm{solute}_3)\mathrm{solute}_2^{n_2} + c_{n_2-1}(\mathrm{solute}_{n-1}, \\ & \mathrm{solute}_{n-2}, \ldots, \mathrm{solute}_3)\mathrm{solute}_2^{n_2^{-1}} + \cdots + c_1(\mathrm{solute}_{n-1}, \mathrm{solute}_{n-2}, \\ & \ldots, \mathrm{solute}_3)\mathrm{solute}_2 + c_0(\mathrm{solute}_{n-1}, \mathrm{solute}_{n-2}, \ldots, \mathrm{solute}_3)\end{aligned} \tag{53}$$

Continuing: and each $c_k(\mathrm{solute}_{n-1}, \mathrm{solute}_{n-2}, \ldots, \mathrm{solute}_3)$, $k = 0$ to n_2 has the form:

$$\begin{aligned}& c_{n_3}(\mathrm{solute}_{n-1}, \mathrm{solute}_{n-2}, \ldots, \mathrm{solute}_4)\mathrm{solute}_3^{n_3} + c_{n_3-1}(\mathrm{solute}_{n-1}, \\ & \mathrm{solute}_{n-2}, \ldots, \mathrm{solute}_4)\mathrm{solute}_3^{n_3-1} + \cdots + c_1(\mathrm{solute}_{n-1}, \\ & \mathrm{solute}_{n-2}, \ldots, \mathrm{solute}_4)\mathrm{solute}_3 + c_0(\mathrm{solute}_{n-1}, \\ & \mathrm{solute}_{n-2}, \ldots, \mathrm{solute}_4)\end{aligned} \tag{54}$$

and each $c_k(\mathrm{solute}_{n-1}, \mathrm{solute}_{n-2})$ were $k = 0$ to $n_{n_{n-3}}$ has the form:

$$\begin{aligned}& c_{n_{n-2}}(\mathrm{solute}_{n-1})\mathrm{solute}_{n-2}^{n_{n-2}} + c_{n_{n-2}-1}(\mathrm{solute}_{n-1})\mathrm{solute}_{n-2}^{n_{n-2}-1} \\ & + \cdots + c_1(\mathrm{solute}_{n-1})\mathrm{solute}_{n-2} + c_0(\mathrm{solute}_{n-1})\end{aligned} \tag{55}$$

Until each $c_k(\mathit{solute}_{n-1})$, where $k = 0$ to n_{n-2}, has the form:

$$\begin{aligned}& c_{k,j}\mathrm{solute}_{n-1}^{j} + c_{k,j-1}\mathrm{solute}_{n-1}^{j-1} + \cdots + c_{k,1}\mathrm{solute}_{n-1} \\ & + c_{k,0}(\mathrm{solute}_{n-1})\end{aligned} \tag{56}$$

where j usually is about 3.

References

[1] L.A.A.E. Sluyterman, O. Elgersma, J. Chromatogr. 150 (1978) 17.
[2] L.A.A.E. Sluyterman, J. Wijdenes, J. Chromatogr. 150 (1978) 31.
[3] L.A.A.E. Sluyterman, J. Wijdenes, J. Chromatogr. 206 (1981) 206.
[4] L.A.A.E. Sluyterman, J. Wijdenes, J. Chromatogr. 206 (1981) 441.
[5] L.A.A.E. Sluyterman, C. Kooistra, J. Chromatogr. 470 (1989) 317.
[6] Y. Liu, D.J. Anderson, J. Chromatogr. A 762 (1997) 47.
[7] Y. Liu, D.J. Anderson, J. Chromatogr. A 762 (1997) 207.
[8] R. Bates, D.D. Frey, J. Chromatogr. A 814 (1998) 43.
[9] K.A. Logan, I. Lagerlund, S.M. Chamow, Biotechnol. Bioeng. 62 (1999) 208.
[10] R.C. Bates, X. Kang, D.D. Frey, J. Chromatogr. A 890 (2000) 25.
[11] X. Kang, R.C. Bates, D.D. Frey, J. Chromatogr. A 890 (2000) 37.
[12] J.W. Rasmussen, N. Høiby, J. Chromatogr. B 746 (2000) 161.
[13] L. Shan, D.J. Anderson, J. Chromatogr. A 909 (2001) 191.
[14] L. Shan, D.J. Anderson, Anal. Chem. 74 (2002) 5641.
[15] X. Kang, D.D. Frey, Anal. Chem. 74 (2002) 1038.
[16] X. Kang, D.D. Frey, J. Chromatogr. A 991 (2003) 117.
[17] T. Andersen, M. Pepaj, R. Trones, E. Lundanes, T. Greibrokk, J. Chromatogr. A 1025 (2004) 217.
[18] L.I. Tsonev, A.G. Hirsh, J. Chromatogr. A 1200 (2008) 166.
[19] L.I. Tsonev, A.G. Hirsh, United States Patent, US 7,425,263 B2, 09.16.2008.
[20] C. Ou, C.L. Rognerud, Cln. Chem. 39 (5) (1993) 820.
[21] P. Wiczling, R. Kaliszan, J. Chromatogr A. 1217 (2010) 3375.
[22] R. Kaliszan, P. Wiczling, M.J. Markuszewski, Anal. Chem. 76 (2004) 749.
[23] P. Wiczling, M.J. Markuszewski, M. Kaliszan, K. Galer, R. Kaliszan, J. Pharm. Biomed. Anal. 37 (2005) 871.
[24] P. Wiczling, M.J. Markuszewski, M. Kaliszan, R. Kaliszan, Anal. Chem. 77 (2005) 449.
[25] J. Ståhlberg, B. Jönsson, Cs. Horváth, Anal. Chem. 63 (1991) 1867.
[26] J. Ståhlberg, B. Jönsson, Anal. Chem. 68 (1996) 1536.
[27] E. Hallgren, F. Kálmán, D. Farnan, C. Horváth, J. Ståhlberg, J. Chromatogr. A 877 (2000) 13.
[28] Swiss-Prot UniProtKB Database: http://www.uniprot.org/uniprot/P01012.
[29] B. Lee, Proc. Natl. Acad. Sci. U.S.A. 80 (1983) 622.
[30] C.N. Pace, G.R. Grimsley, J.M. Scholtz, J. Biol. Chem. 284 (20) (2009) 13285.